Journal of Anesthesia (2024) 38:44–56
https://doi.org/10.1007/s00540-023-03271-8

ORIGINAL ARTICLE

Alleviated cerebral infarction in male mice lacking all nitric oxide synthase isoforms after middle cerebral artery occlusion

Haruaki Kubota[1,2] · Masato Tsutsui[1] · Kanako Kuniyoshi[1] · Hirotaka Yamashita[1] · Hiroaki Shimokawa[3,4] · Kazuhiro Sugahara[2] · Manabu Kakinohana[2]

Received: 1 December 2022 / Accepted: 5 October 2023 / Published online: 1 November 2023

Abstract

Purpose The role of the nitric oxide synthases (NOSs) system in cerebral infarction has been examined in pharmacological studies with non-selective NOSs inhibitors. However, due to the non-specificity of the non-selective NOSs inhibitors, its role remains to be fully elucidated. We addressed this issue in mice in which neuronal, inducible, and endothelial NOS isoforms were completely disrupted.

Methods and results We newly generated mice lacking all three NOSs by crossbreeding each single NOS$^{-/-}$ mouse. In the male, cerebral infarct size at 24 h after middle cerebral artery occlusion (MCAO) was significantly smaller in the triple n/i/eNOSs$^{-/-}$ genotype as compared with wild-type genotype. Neurological deficit score and mortality rate were also significantly lower in the triple n/i/eNOSs$^{-/-}$ than in the WT genotype. In contrast, in the female, there was no significant difference in the cerebral infarct size in the two genotypes. In the male triple n/i/eNOSs$^{-/-}$ genotype, orchiectomy significantly increased the cerebral infarct size, and in the orchiectomized male triple n/i/eNOSs$^{-/-}$ genotype, treatment with testosterone significantly reduced it. Cyclopaedic and quantitative comparisons of mRNA expression levels in cerebral infarct lesions between the male wild-type and triple n/i/eNOSs$^{-/-}$ genotypes at 1 h after MCAO revealed significant involvements of decreased oxidative stress and mitigated mitochondrial dysfunction in the alleviated cerebral infarction in the male triple n/i/eNOSs$^{-/-}$ genotype.

Conclusions These results provide the first evidence that the NOSs system exerts a deleterious effect against acute ischemic brain injury in the male.

Keywords Cerebral infarction · Mice · Nitric oxide synthase · Sex difference · Testosterone

Introduction

Stroke is a serious life-threatening medical condition that stenosis, obstruction, or rupture of cerebral blood vessels causes abrupt brain tissue injury, resulting in sudden onset of headache, dizziness, and neurological symptoms, including impaired consciousness, motor-sensory disturbance, dysphasia, and anopsia [1, 2]. Stroke includes cerebral infarction, cerebral hemorrhage, and subarachnoid hemorrhage. World Health Organization's Global Health Estimates reported in 2020 that stroke is the second-most common cause of death, responsible for 11% (6.1 million deaths) of the world's total deaths (55.4 million deaths), and that stroke is the leading cause of physical disability worldwide (https://www.who.int/news-room/fact-sheets/detail/the-top-10-causes-of-death). An increase in burden of nursing-care that is induced by cognitive impairment after developing stroke is also a major medical problem. Cerebral infarction accounts for approximately 60% of stroke. Hypertension, arrythmia (atrial fibrillation), diabetes mellitus, smoking, obesity, and metabolic syndrome are major risk factors of cerebral infarction. Because cerebral infarction leaves serious sequelae even if patients with cerebral infarction escape

✉ Masato Tsutsui
tsutsui@med.u-ryukyu.ac.jp

1 Department of Pharmacology, Graduate School of Medicine, University the Ryukyus, 207 Uehara, Nishihara, Okinawa 903-0215, Japan

2 Department of Anesthesiology, Graduate School of Medicine, University the Ryukyus, Nishihara, Okinawa, Japan

3 Department of Cardiovascular Medicine, Tohoku University Graduate School of Medicine, Sendai, Japan

4 Graduate School, International University of Health and Welfare, Narita, Japan

death, the establishment of effective therapy is of crucial importance. However, since the precise pathogenesis of cerebral infarction has not been fully elucidated, its definitive therapeutic strategies have yet to be developed [1, 2].

Nitric oxide (NO) plays an important role in maintaining homeostasis of the central nervous system. NO is a gaseous free radical, freely passes through plasma membranes, and elicits multiple actions without receptor coupling. The NO synthase system consists of three distinct isoforms, including neuronal (nNOS), inducible (iNOS), and endothelial NOS (eNOS) [3–5]. All three NOS isoforms have been reported to be expressed in cerebral infarct lesions [6–8]. In a mouse middle cerebral artery occlusion (MCAO) model, as compared with wild-type (WT) mice, eNOS$^{-/-}$ mice show larger cerebral infarct size [6], whereas nNOS$^{-/-}$ [7] and iNOS$^{-/-}$ mice [8] conversely exhibit smaller cerebral infarct size. These results indicate a distinct role of each NOS isoform in cerebral infarction. The role of the whole NOSs system in cerebral infarction has been examined in pharmacological studies with non-selective NOSs inhibitors, such as N^{ω}-nitro-L-arginine (L-NNA) or N^{ω}-nitro-L-arginine methyl ester (L-NAME). However, the pharmacological studies have yielded conflicting results, as reported that, in a rat MCAO model, treatment with L-NNA increases cerebral infarct size [9], whereas treatment with L-NAME conversely reduces it [10]. This inconsistency would be due to the non-specificity of the non-selective NOSs inhibitors [11, 12]. To overcome this issue, in the present study, we newly generated mice deficient in all three NOS isoforms, and investigated the role of the entire NOSs system in the pathogenesis of cerebral infarction by the use of this triple mutant mouse.

Methods

This study was approved by the Animal Care and Use Committee, the University of the Ryukyus, Japan.

Animal preparation

We previously generated triple n/i/eNOSs$^{-/-}$ mice by cross-breeding each single NOS$^{-/-}$ mice [13]. There are three different iNOS$^{-/-}$ mice made by three different research groups [5]. In this study, by using another iNOS$^{-/-}$ mice [14], we newly created triple n/i/eNOSs$^{-/-}$ mice. Eight- to twelve-week-old triple n/i/eNOSs$^{-/-}$ and WT littermate mice of both sexes were used. All the mice were maintained in temperature- and humidity-controlled rooms illuminated from 08:00 to 20:00 h. Genotype for the NOS genes was determined by polymerase chain reaction (PCR) with tail genomic DNA [13].

Cerebrovascular anatomy

Cerebrovascular anatomy was examined by carbon black perfusion as previously described [15]. In brief, a lethal dose of papaverine hydrochloride (40–50 mg/kg in sterile water) was injected intravenously immediately before latex infusion to produce maximal vasodilation and to facilitate vascular filling. The thoracic aorta was clipped at the level of the diaphragm and cannulated with a polyethylene tubing (internal diameter 0.58 mm, Becton Dickinson, MD, USA). Warm (38 °C) undiluted latex (L-5000, Qua-Yu-Kasei Ltd., Yamato, Japan) was mixed well with a small amount of carbon black (Bokusai, Fueki, Tokyo, Japan) and it was injected into the aorta. The injection volume of latex was 0.5 ml and the duration of injection was about 10 s. At 30 min after the injection, the animals were decapitated, and the brains were carefully removed and placed in 10% formalin.

Anastomoses of cerebral arteries were analyzed on a photograph by tracing the peripheral branches of the anterior cerebral artery and the middle cerebral artery to the points of anastomoses, defined as the narrowest vessel diameter or the half distance between the nearest branching points of the anterior cerebral artery branches and the middle cerebral artery branches, respectively [16]. Adjacent anastomotic points were connected to identify the line of anastomoses [17], which represents the border of the supplying territories of the anterior cerebral artery and the middle cerebral artery. The distances from the midline to the line of anastomoses were measured in a coronal plane at 2, 4, and 6 mm from the frontal pole [15].

MCAO and assessment of cerebral infarction

Mice were anesthetized with isoflurane inhalation. Body temperature was monitored with a rectal probe and maintained at approximately 37 °C by a heating pad (ATC-210; Unique Medical, Tokyo, Japan). Focal cerebral ischemia was induced by MCAO by an intraluminal filament technique [18, 19]. A silicon-covered nylon filament (8-0) was introduced via the common carotid artery towards the middle cerebral artery. In a transient MCAO model, the filament was placed in the middle cerebral artery for 1 h, followed by 23 h of reperfusion, and in a permanent MCAO model, the filament was placed for 24 h without reperfusion. Cerebral blood flow was monitored using a laser Doppler flowmeter (FLO-C1, Omegawave Inc., Tokyo, Japan). In some mice, the right common carotid artery was cannulated for systemic arterial blood gas sampling under mechanical ventilation with isoflurane anesthesia (5.0% for intubation and 2.0% during surgery).

PaO_2, $PaCO_2$, SaO_2 and pH in arterial blood samples were measured with a blood analyzer (i-STAT; Abbott, IL). Neurological deficits of animals were assessed at 24 h after MCAO as previously reported [20]. After that, the brain was removed and sectioned coronally into 2-mm slices using a mouse brain matrix (Muromachi, Tokyo, Japan). The sections were immediately stained with a 2% 2,3,5-triphenyltetrazolium chloride (TTC) solution at 37 °C for 20 min. The border between infarcted and non-infarcted tissues was outlined using an Image J software (National Institute of Health, Bethesda, MD) and infarct area was measured by subtracting the area of the non-lesioned ipsilateral hemisphere from that of the contralateral hemisphere [21]. Infarct volume was calculated by integration of the infarct areas at five equidistant levels of the forebrain.

Ovariectomy (OVX) and orchiectomy (ORX)

Bilateral OVX, bilateral ORX, or sham-operation was performed in 7–11-week-old WT mice under general anesthesia with an intraperitoneal injection of mixed anesthetics of midazolam (4 mg/kg), medetomidine hydrochloride (0.75 mg/kg) and butorphanol tartrate (5 mg/kg) at 1 week before MCAO. In rescue experiments, either testosterone-filled silicone tube or empty tube was implanted subcutaneously in the back of orchiectomized mice. Plasma levels of testosterone were assessed with an ELISA kit (Cayman chemical, Ann Arbor, MI, USA).

Peroxynitrite

Oxidative stress was estimated by measuring nitrotyrosine levels in mouse brains (infarct and non-infarct hemispheres) by Western blot analysis [22, 23]. Membrane was immunoblotted with anti-nitrotyrosine (Merck Millipore, Billerica, MA, USA) and anti-glyceraldehyde 3-phosphate dehydrogenase (GAPDH) antibodies (Sigma-Aldrich). After incubating with horseradish peroxidase-conjugated anti-rabbit IgG antibodies (Cell Signaling Technology, Danvers, MA, USA), blots were visualized by an enhanced chemiluminescence system (ECL Prime Western Blotting Detection Reagent, GE Healthcare, Little Chalfont, UK), scanned with a luminoimage analyzer (LAS-4000 mini, Fuji Film, Tokyo, Japan), and analyzed with a multi-gauge software (Fuji Film).

RNA sequencing

The brain was isolated and quickly immersed in an RNA stabilization reagent (RNase later, QIAGEN, Valencia, CA) at 1 h after transient MCAO. It was then homogenized in Qiazol (QIAGEN) with a homogenizer (Power Masher II, Nippi, Tokyo, Japan), and total RNA was extracted from the homogenized mixture with a miRNeasy mini kit (QIAGEN). In 8 individual samples (4 from the cerebral infarct lesions of the male WT mice and 4 from those of the male triple n/i/eNOSs$^{-/-}$ mice), total RNA concentrations were determined by a spectrophotometer (NanoDrop 2000, Thermo Scientific, Wilmington, DE), and the quality of the total RNA samples was assessed by an Agilent 2100 Bioanalyzer (Agilent Technologies, Palo Alto, CA). mRNA was extracted with a Dynabeads mRNA Purfication Kit (Thermo,Waltham, MA), and cDNA was generated from 500 ng of mRNA using a PrimeScript Double Strand cDNA Synthesis Kit (Takara Bio, Otsu, Japan). Fifty ng of each cDNA sample was sheared in 200–500 bp using a Covaris S220 (Covaris, Woburn, MA), and 75 bp single-end reads were prepared using KAPA Library Preparation Kits (Kapa Biosystems, Wilmington, MA). The cDNA libraries were indexed for multiplexing, and were sequenced on an Illumina HiSeq 2500 platform as previously reported [24]. Mean mRNA expression levels in the WT mice and triple n/i/eNOSs$^{-/-}$ mice that were up- or down-regulated greater than 1.2-fold were statistically analyzed.

Statistical analyses

Results are expressed as means ± SEM. The data were analyzed by a Student's *t* test, an analysis of variance (ANOVA) followed by a Bonferroni's test, or a fisher exact test. We used Graph Pad Prism Version 7.0 (Graph Pad Software Inc., San Diego, CA.), Subio Platform (Subio, Kagoshima, Japan), Ingenuity Pathway Analysis (IPA, QIAGEN), and the Database for Annotation, Visualization, and Integrated Discovery (DAVID) (v6.8). A value of $P < 0.05$ was considered to be statistically significant.

Results

Generation of triple n/i/eNOSs$^{-/-}$ mice

We newly generated triple n/i/eNOSs$^{-/-}$ mice by crossing nNOS$^{-/-}$, iNOS$^{-/-}$, and eNOS$^{-/-}$ mice. We first studied whether or not cerebrovascular anatomy is similar in WT littermates and triple n/i/eNOSs$^{-/-}$ mice by carbon black perfusion. Appearances of cerebrovascular structure were comparable between male WT and male triple n/i/eNOSs$^{-/-}$ mice (Fig. 1A) and between male and female triple n/i/eNOSs$^{-/-}$ mice (Fig. 1B). Quantitative evaluations of the distance of the line of cerebral artery anastomoses from the midline also indicated no statistically significant difference in cerebral angioarchitecture between the male WT and male triple n/i/eNOSs$^{-/-}$ mice (Fig. 1C). There was

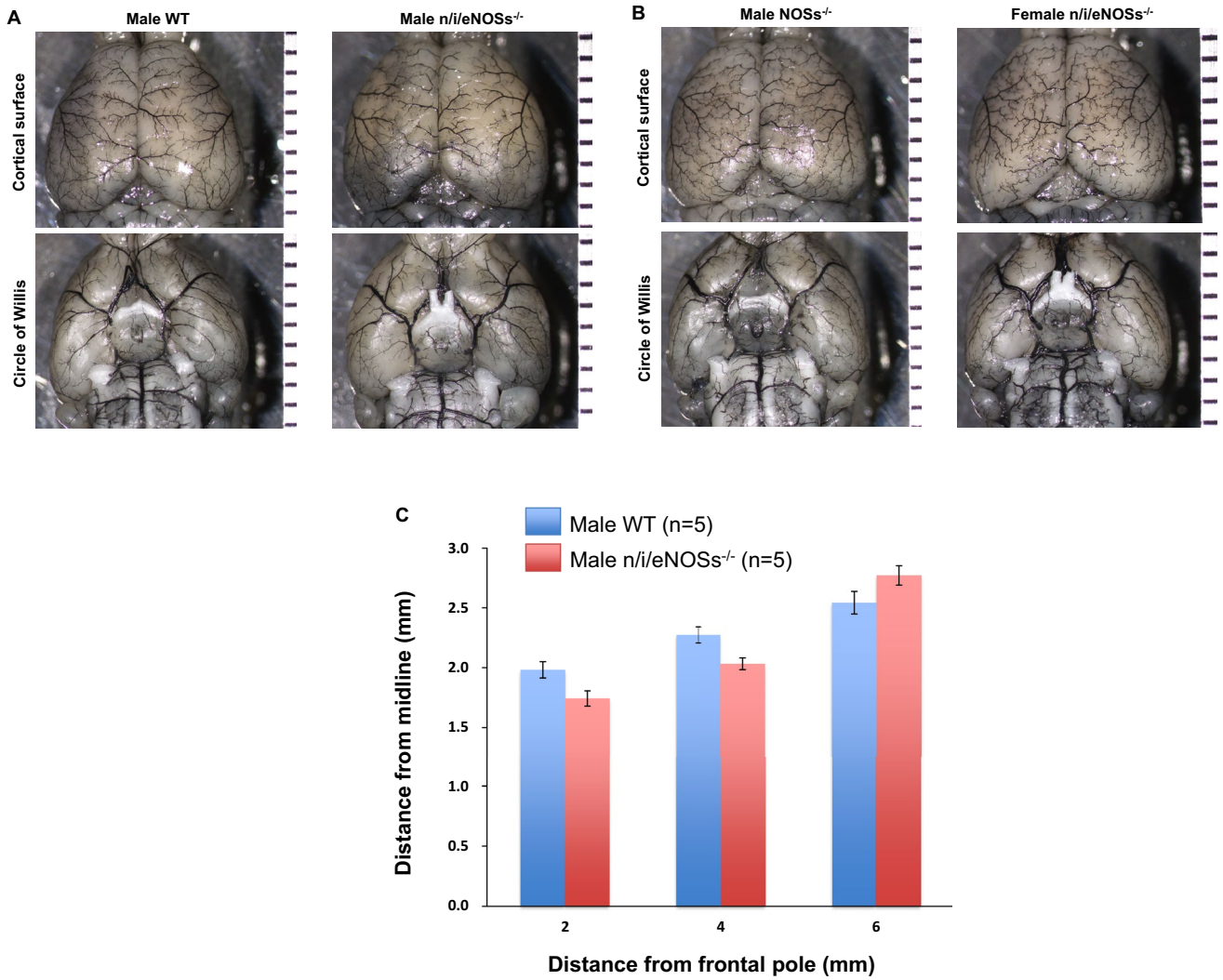

Fig. 1 Similar cerebrovascular structure in wild-type (WT) and triple n/i/eNOSs$^{-/-}$ mice examined by carbon black perfusion. **A** Cerebrovascular structure in male WT and triple n/i/eNOSs$^{-/-}$ mice. **B** Cerebrovascular structure in male and female triple n/i/eNOSs$^{-/-}$ mice. **C** The distance of the line of cerebral artery anastomoses from the midline in male WT and triple n/i/eNOSs$^{-/-}$ mice ($n=5$ each). The data were analyzed by ANOVA

no significant difference in body weight in the two genotypes (data not shown).

Reductions of cerebral infarct size, neurological deficit score, and mortality rate in male triple n/i/eNOSs$^{-/-}$ mice after MCAO

Figure 2A shows representative pictures of TTC staining of 2 mm-thick brain slices in the male WT and triple n/i/eNOSs$^{-/-}$ mice at 24 h after 1 h transient MCAO. Cerebral infarct size after the transient MCAO was markedly reduced in the male triple n/i/eNOSs$^{-/-}$ mice as compared with the male WT mice (white color in Fig. 2A). Quantitative analyses indicated that cerebral infarct area in each brain slice (Fig. 2B) and cerebral infarct volume estimated from the cerebral infarct area (Fig. 2C) were both significantly smaller in the male triple n/i/eNOSs$^{-/-}$ than in the male WT mice. Neurological deficit score (Fig. 2D) and mortality rate (Fig. 2E) after the transient MCAO were also significantly lower in the male triple n/i/eNOSs$^{-/-}$ than in the male WT mice. None of 10 triple n/i/eNOSs$^{-/-}$ mice studied died after the transient MCAO (Fig. 2E). There were no significant differences in the arterial blood gas data of PaO_2, $PaCO_2$, SaO_2 and pH under mechanical ventilation with isoflurane anesthesia in the two genotypes (data not shown).

Ischemic strokes are categorized by transient or permanent obstruction of cerebral blood flow. Experimental transient and permanent MCAO models target different stroke patients in the clinical scenario, and the two MCAO models

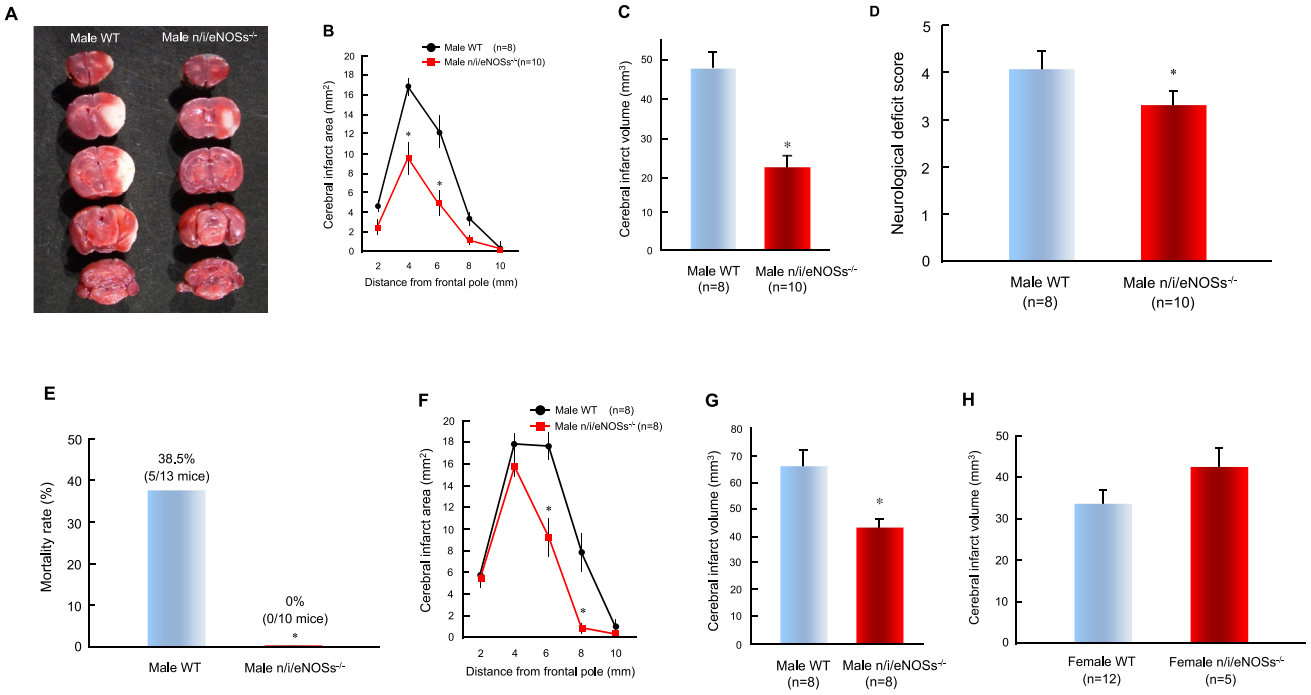

Fig. 2 Decreases of cerebral infarct size, neurological deficit score, and mortality rate in male triple n/i/eNOSs$^{-/-}$ mice and no change of cerebral infarct size in female triple n/i/eNOSs$^{-/-}$ mice after middle cerebral artery occlusion (MCAO). **A** TTC staining of 2 mm-thick brain slices in male WT and triple n/i/eNOSs$^{-/-}$ mice at 24 h after transient MCAO. White color indicates cerebral infarct lesions. **B** Cerebral infarct area in each brain slice. **C** Cerebral infarct volume calculated from the results of the cerebral infarct area. **D** Neurological deficit score. **E** Mortality rate. **F**, **G** Cerebral infarct area in each brain slice and cerebral infarct volume in male WT and triple n/i/eNOSs$^{-/-}$ mice at 24 h after permanent MCAO. $*P<0.05$ versus WT mice. **H** Cerebral infarct volume in female WT and triple n/i/eNOSs$^{-/-}$ mice at 24 h after transient MCAO. The data were analyzed by Student's *t* test (**C**, **D**, **G**, **H**), ANOVA followed by Bonferroni's test (**B**, **F**), and by Fisher exact test (**E**)

show marked differences in histopathological changes and various pathophysiological processes, such as neuronal apoptosis, neuroinflammation, and oxidative stress [25]. Thus, we next carried out permanent MCAO for 24 h. The cerebral infarct area (Fig. 2F) and the cerebral infarct volume (Fig. 2G) after the permanent MCAO were also significantly smaller in the male triple n/i/eNOSs$^{-/-}$ than in the male WT mice as in the case of the transient MCAO. Four out of twelve male WT mice and four out of twelve triple male n/i/eNOSs$^{-/-}$ mice died after the permanent MCAO. Based on these results, the transient MCAO was performed in the following experiments.

Sex difference in cerebral infarct size in triple n/i/eNOSs$^{-/-}$ mice after transient MCAO

We then examined whether or not sex difference is present in the cerebral infarct size of triple n/i/eNOSs$^{-/-}$ mice after the transient MCAO. In contrast to the male WT and triple n/i/eNOSs$^{-/-}$ mice, there was no significant difference in the cerebral infarct volume in female WT and triple n/i/eNOSs$^{-/-}$ mice after the transient MCAO, and the cerebral infarct volume rather tended to be larger in the female triple n/i/eNOSs$^{-/-}$ than in the female WT mice (Fig. 2H). Two out of fourteen female WT mice and none of five female n/i/eNOSs$^{-/-}$ mice died after the transient MCAO.

We then examined the mechanism of this sex difference by OVX or ORX. In the female triple n/i/eNOSs$^{-/-}$ mice, OVX did not significantly affect the cerebral infarct volume as compared with sham-operation (Fig. 3A). In the male triple n/i/eNOSs$^{-/-}$ mice, ORX significantly increased the cerebral infarct volume compared with the sham-operation (Fig. 3C), and in the orchiectomized male triple n/i/eNOSs$^{-/-}$ mice, treatment with testosterone significantly reduced it (Fig. 3E). On the other hand, in the male WT mice, ORX conversely significantly decreased the cerebral infarct volume compared with the sham-operation (Fig. 3B), and in the orchiectomized male WT mice, testosterone treatment significantly increased it (Fig. 3D).

Mechanisms of reduced cerebral infarct size in male triple n/i/eNOSs$^{-/-}$ mice after transient MCAO

To clarify the mechanisms of reduced cerebral infarct size in the male triple n/i/eNOSs$^{-/-}$ mice after the transient MCAO, we measured cerebral blood flow by a laser Doppler

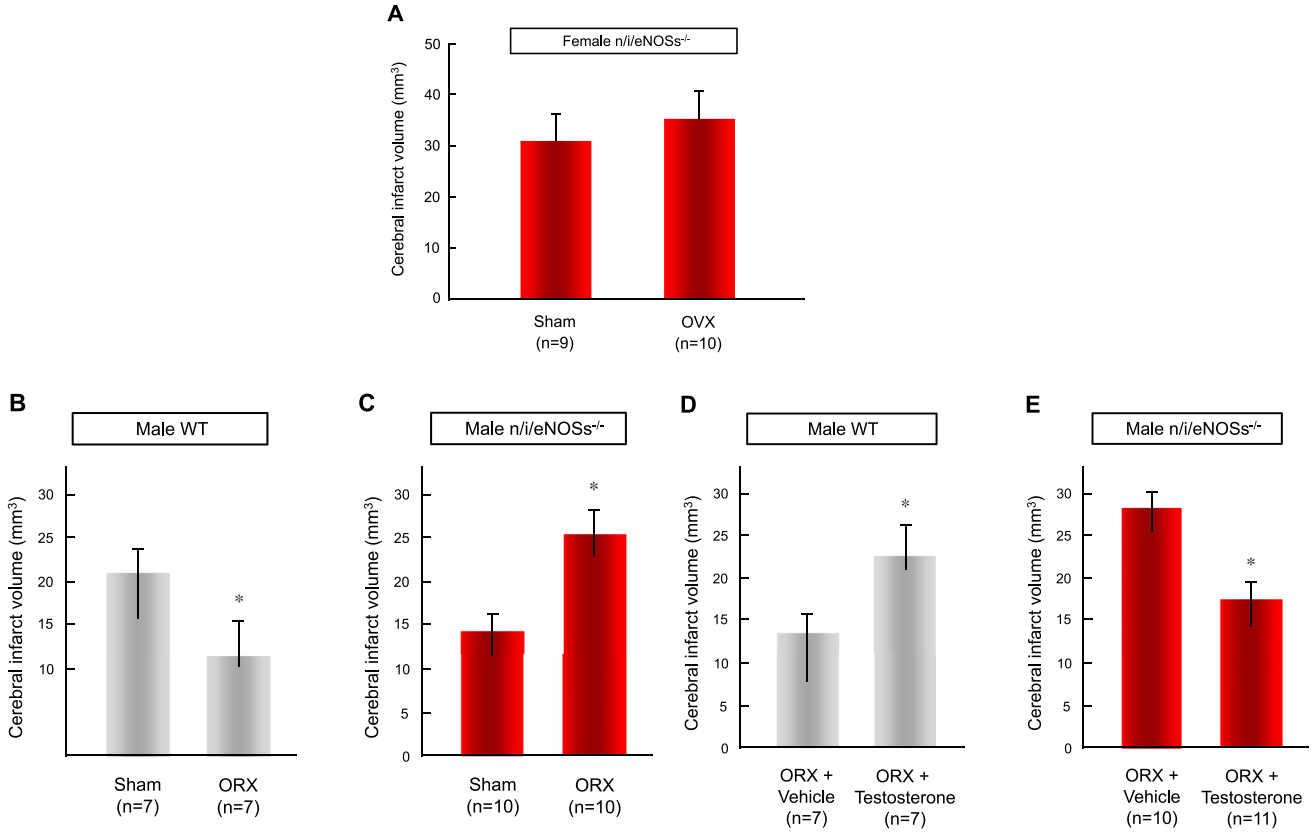

Fig. 3 Effects of ovariectomy (OVX), orchiectomy (ORX), and testosterone treatment on cerebral infarct size in WT and triple n/i/eNOSs$^{-/-}$ mice after transient MCAO. **A** An effect of OVX on cerebral infarct volume in female triple n/i/eNOSs$^{-/-}$ mice. **B**, **C** Effects of ORX on cerebral infarct volume in male WT and triple n/i/eNOSs$^{-/-}$ mice. **D**, **E** Effects of subcutaneous testosterone treatment on cerebral infarct volume in male WT and triple n/i/eNOSs$^{-/-}$ mice that underwent ORX. *$P < 0.05$ versus WT mice. The data were analyzed by Student's *t* test (**A**–**E**)

flowmeter. The cerebral blood flow at baseline and during the MCAO was comparable in the male WT and triple n/i/eNOSs$^{-/-}$ mice, but that during reperfusion was significantly lower in the male triple n/i/eNOSs$^{-/-}$ mice as compared with the male WT mice (Fig. 4).

We next examined the molecular mechanisms by RNA sequencing. We assessed mRNA expression levels in the cerebral infarct lesions of the male WT and triple n/i/eNOSs$^{-/-}$ mice at 1 h after MCAO (each $n = 4$). Both the canonical pathway analysis and the tox list analysis indicated a significant involvement of oxidative stress and mitochondrial dysfunction (Fig. 5A, B). mRNA levels of 16 genes that are related to oxidative stress were differentially expressed (Table 1) and in the cerebral infarct lesions of the male triple n/i/eNOSs$^{-/-}$ mice as compared with the male WT mice, representative genes that promote oxidative stress, such as peroxiredoxin-6, intercellular adhesion molecule 1 (ICAM1), vascular cell adhesion molecule 1 (VCAM1), glutathione S-transferase, glutathione peroxidase 7, and high mobility group box 1 (HMGB1), were significantly down-regulated (Fig. 5C). In addition, mRNA levels of 44 genes that are related to mitochondrial dysfunction were differentially expressed (Table 2) and in the cerebral infarct lesions of the male triple NOSs$^{-/-}$ mice as compared with the male WT mice, representative genes that augment mitochondrial dysfunction, such as cytochrome c, caspase 8, presenilin 2 (PSEN2), and presenilin enhancer (PSENEN), were significantly down-regulated, and representative genes that inhibit mitochondrial dysfunction, such as B-cell/CLL lymphoma 2 (BCL2) and PTEN-induced putative kinase 1 (PINK1), were significantly up-regulated (Fig. 5D).

Since the results of the RNA sequencing suggest an involvement of decreased oxidative stress, we further examined nitrotyrosine levels, a marker of oxidative stress. In the male WT mice, the nitrotyrosine levels were significantly higher in the cerebral infarct lesions than in non-cerebral infarct regions of contralateral unaffected hemisphere (Fig. 6A), whereas in the male triple n/i/eNOSs$^{-/-}$ mice, this change was modest and did not reach a statistically significant level (Fig. 6A). When the nitrotyrosine levels in the cerebral infarct lesions were compared between both genotypes, they were significantly lower in the male triple n/i/

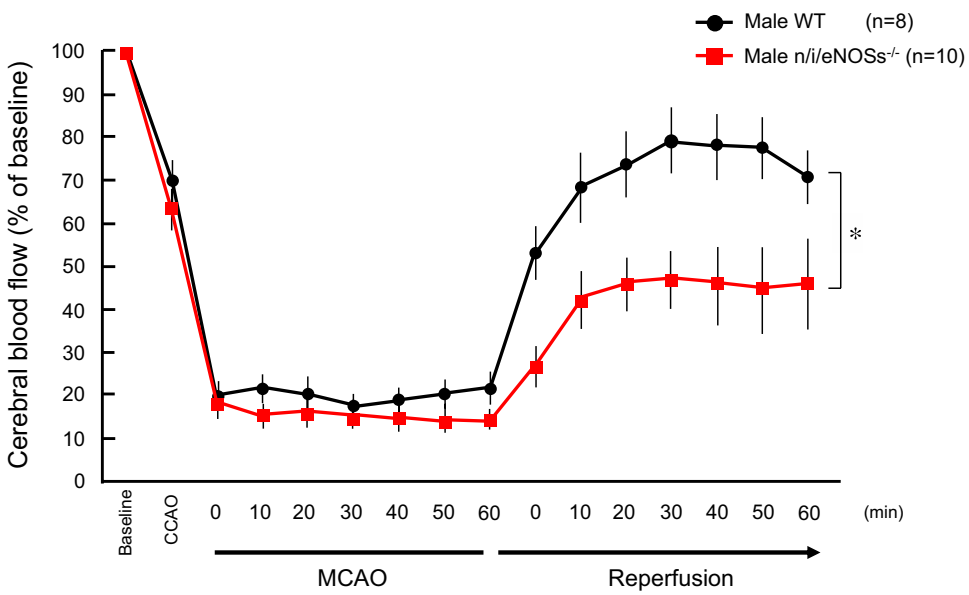

Fig. 4 Cerebral blood flow in male WT and triple n/i/eNOSs$^{-/-}$ mice at baseline and during and after MCAO measured by laser Doppler flowmeter. *$P < 0.05$ versus WT mice. CCAO: common carotid artery occlusion. The data were analyzed by ANOVA

eNOSs$^{-/-}$ than in the male WT mice (Fig. 6A). In the female WT mice, a modest increase in the nitrotyrosine levels were observed in the cerebral infarct lesions as compared with the non-cerebral infarct regions (Fig. 6B) and there was no significant difference in the nitrotyrosine levels in the cerebral infarct lesions between the female WT and the female triple n/i/eNOSs$^{-/-}$ mice (Fig. 6B).

Discussion

Alleviated cerebral infarction in triple n/i/eNOSs$^{-/-}$ mice after MCAO

In the present study, we newly generated mice deficient in all three NOS isoforms. No structural abnormality of cerebral blood vessels was noted in the triple n/i/eNOSs$^{-/-}$ mice as compared with the WT mice, and the body weight was comparable in the two genotypes. The male triple n/i/eNOSs$^{-/-}$ mice manifested decreases in cerebral infarct size, neurological deficit score, and mortality rate as compared with the male WT mice after the transient MCAO. They similarly displayed a decrease in cerebral infarct size after the permanent MCAO as in the case of the transient MCAO. These results suggest that the whole NOSs system plays a deleterious role in the pathogenesis of cerebral infarction irrespective of transient or sustained cerebral ischemia. It has been reported that neuronal NO overproduction derived from nNOS [7] and iNOS [8] exacerbates acute ischemic brain injury after the transient MCAO, whereas vascular NO production derived from eNOS protects it [6]. Our findings demonstrate that NO production derived from all three NOSs leads to neurotoxicity in acute ischemic brain injury.

Sex difference in cerebral infarction in triple n/i/eNOSs$^{-/-}$ mice after transient MCAO

In contrast to the male mice, the cerebral infarct size rather tended to be larger in the female triple n/i/eNOSs$^{-/-}$ than in the female WT mice after the transient MCAO, indicating the presence of sex difference in the cerebral infarct size in the triple n/i/eNOSs$^{-/-}$ mice. In the WT genotype, the cerebral infarct size was larger in the male than in the female, whereas in the triple n/i/eNOSs$^{-/-}$ genotype, it was conversely smaller in the male than in the female. In the female triple n/i/eNOSs$^{-/-}$ genotype, OVX did not affect the cerebral infarct volume as compared with the sham-operation. On the other hand, in the male triple n/i/eNOSs$^{-/-}$ genotype, ORX increased the cerebral infarct volume compared with the sham-operation, and in the orchiectomized male triple n/i/eNOSs$^{-/-}$ genotype, treatment with testosterone significantly reduced it, indicating a protective effect of testosterone against acute cerebral ischemia in the absence of NOSs. It is thus possible that testosterone is involved in the reduced cerebral infarct size in the male triple n/i/eNOSs$^{-/-}$ mice after the transient MCAO. On the contrary, in the male WT genotype, ORX decreased the cerebral infarct volume compared with the sham-operation, and in the orchiectomized male WT mice, testosterone treatment significantly increased it. In agreement with these results, testosterone has been reported to increase the cerebral infarct size in normal male rats after the transient MCAO [26]. These results suggest for the first time that testosterone exerts a deleterious neurotoxic effect under a physiological condition, whereas it

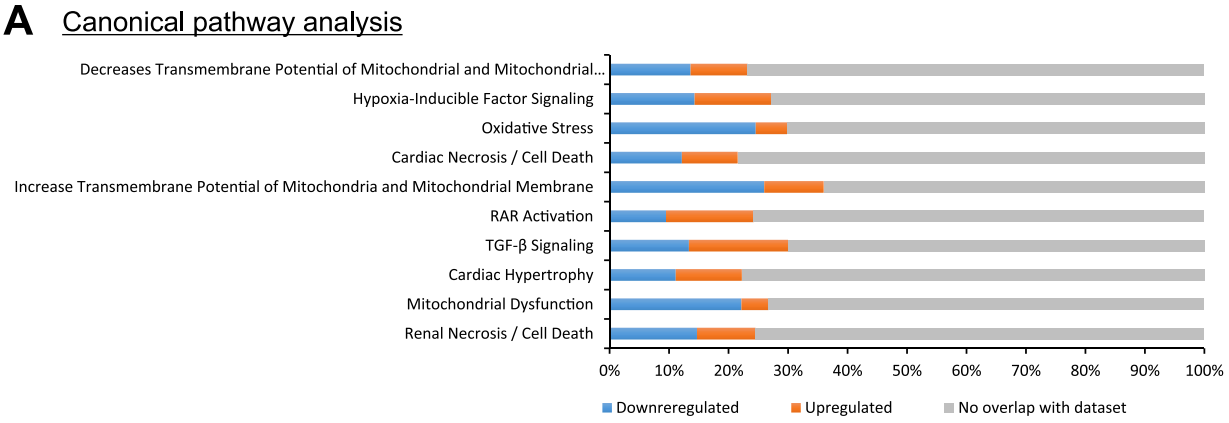
A
Canonical pathway analysis
Decreases Transmembrane Potential of Mitochondrial and Mitochondrial...
Hypoxia-Inducible Factor Signaling
Oxidative Stress
Cardiac Necrosis / Cell Death
Increase Transmembrane Potential of Mitochondria and Mitochondrial Membrane
RAR Activation
TGF-β Signaling
Cardiac Hypertrophy
Mitochondrial Dysfunction
Renal Necrosis / Cell Death
0% 10% 20% 30% 40% 50% 60% 70% 80% 90% 100%
Downreregulated
Upregulated
No overlap with dataset

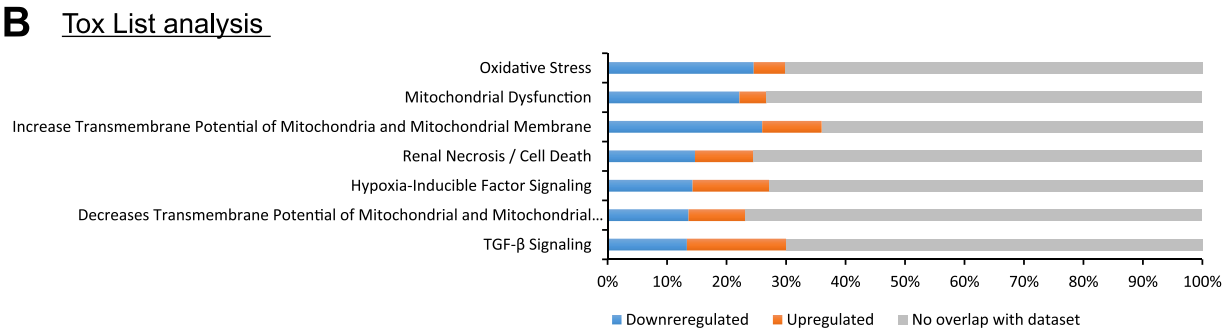
B
Tox List analysis
Oxidative Stress
Mitochondrial Dysfunction
Increase Transmembrane Potential of Mitochondria and Mitochondrial Membrane
Renal Necrosis / Cell Death
Hypoxia-Inducible Factor Signaling
Decreases Transmembrane Potential of Mitochondrial and Mitochondrial...
TGF-β Signaling
0% 10% 20% 30% 40% 50% 60% 70% 80% 90% 100%
Downreregulated
Upregulated
No overlap with dataset

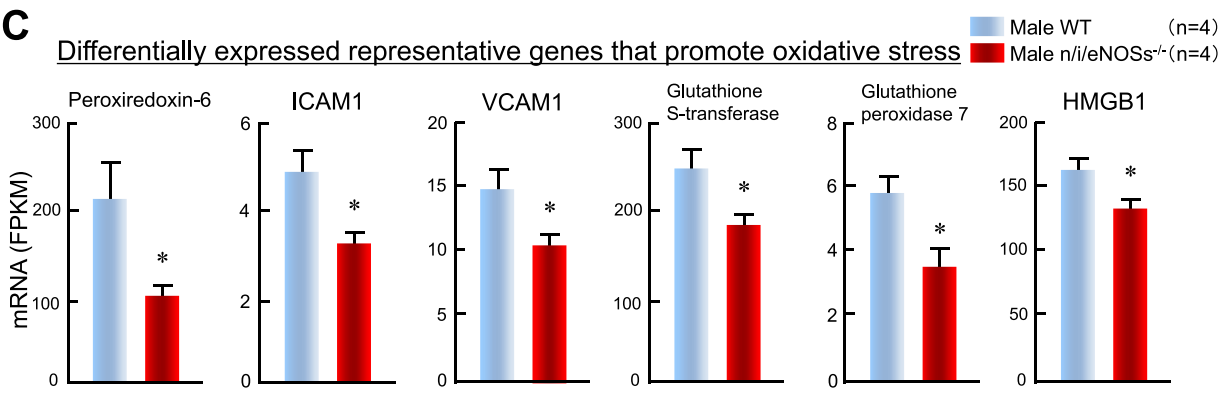
C
Differentially expressed representative genes that promote oxidative stress
Male WT (n=4)
Male n/i/eNOSs-/- (n=4)
Peroxiredoxin-6
ICAM1
VCAM1
Glutathione S-transferase
Glutathione peroxidase 7
HMGB1
mRNA (FPKM)

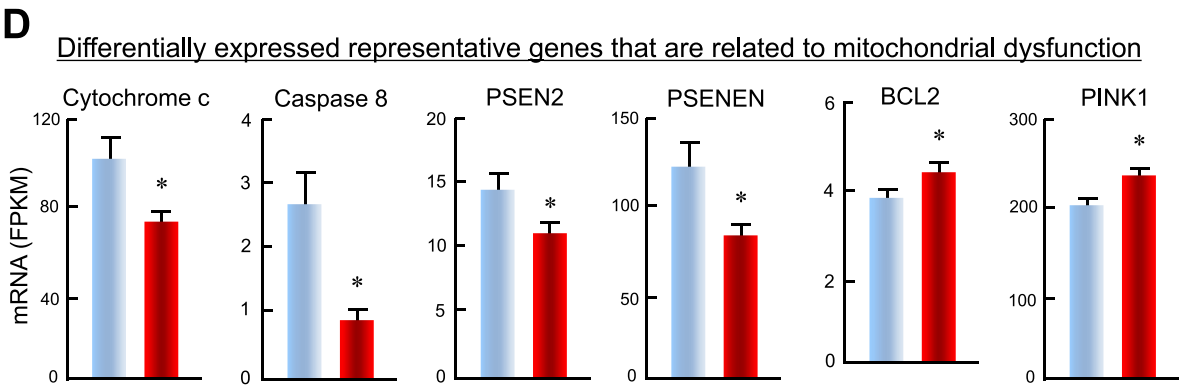
D
Differentially expressed representative genes that are related to mitochondrial dysfunction
Cytochrome c
Caspase 8
PSEN2
PSENEN
BCL2
PINK1
mRNA (FPKM)

◂**Fig. 5** RNA sequencing in cerebral infarct lesions in male WT and triple n/i/eNOSs$^{-/-}$ mice at 1 h after MCAO ($n=4$ each). **A** Canonical pathway analysis. **B** Tox list analysis. **C** Differentially expressed representative genes that promote oxidative stress. **D** Differentially expressed representative genes that are related to mitochondrial dysfunction. *$P<0.05$ versus WT mice. The data were analyzed by Fisher exact test (**A**, **B**) and Student's *t* test (**C**, **D**)

exerts a beneficial neuroprotective effect under a pathological NOSs-deficient condition.

A minor role of attenuated cerebral blood flow in alleviated cerebral infarction in male triple n/i/eNOSs$^{-/-}$ mice after transient MCAO

We next examined the underlying mechanisms of the reduced cerebral infarct size in the male triple n/i/eNOSs$^{-/-}$ mice after the transient MCAO. The cerebral blood flow during reperfusion after the transient MCAO was attenuated in the male triple n/i/eNOSs$^{-/-}$ mice as compared with the male WT mice. This result could be due to vascular eNOS deficiency because the eNOS$^{-/-}$ mice exhibit a similar cerebral blood flow reduction after the transient MCAO [6]. It has been reported that the eNOS$^{-/-}$ mice with reduced cerebral blood flow after the transient MCAO show enlarged cerebral infarct size [6], and that the nNOS$^{-/-}$ [7] and iNOS$^{-/-}$ mice [8] with normal cerebral blood flow after the transient MCAO display decreased cerebral infarct size. It is thus likely that alterations of the cerebral blood flow play a minor role in the determination of the cerebral infarct size after the transient MCAO.

Possible involvements of decreased oxidative stress and reduced mitochondrial dysfunction in alleviated cerebral infarction in male triple n/i/eNOSs$^{-/-}$ mice after transient MCAO

We made cyclopedic and quantitative comparisons of mRNA expression levels in the cerebral infarct lesions of the male WT and triple n/i/eNOSs$^{-/-}$ mice at 1 h after the MCAO by RNA sequencing. The RNA sequencing has high quantitative performance that is comparable to real-time PCR ("gold standard" of mRNA quantitation methods) with 94% of quantitative concordance rate [27]. Both the canonical pathway analysis and the tox list analysis indicated a significant involvement of oxidative stress and mitochondrial dysfunction. Genes that promote oxidative stress, such as peroxiredoxin-6, ICAM1, VCAM1, glutathione S-transferase, glutathione peroxidase 7, and HMGB1 [28, 29], were down-regulated in the cerebral infarct lesions of the male triple NOSs$^{-/-}$ mice as compared with the male WT mice. In addition, in the cerebral infarct lesions of the male triple NOSs$^{-/-}$ mice as compared with the male WT mice, genes that augment mitochondrial dysfunction, such as cytochrome c, caspase 8, PSEN2, and PSENEN [29, 30], were down-regulated, and genes that inhibit mitochondrial dysfunction, such as BCL2 and PINK1 [29, 30], were up-regulated.

Table 1 Differentially expressed genes that are related to oxidative stress

Symbol	Gene name	*P* value	Fold change
BRCA1	BRCA1, DNA repair associated	0.0272	− 1.8
CAT	Catalase	0.000862	− 1.216
DUSP1	Dual specificity phosphatase 1	0.00877	1.393
GSTM1	Glutathione S-transferase mu 1	0.0111	− 4.169
ICAM1	Intercellular adhesion molecule 1	0.00954	− 1.361
JUN	Jun proto-oncogene, AP-1 transcription factor subunit	0.0401	1.605
MAPK14	Mitogen-activated protein kinase 14	0.0169	1.197
NFE2L2	Nuclear factor, erythroid 2 like 2	0.00838	− 1.458
NFKB2	Nuclear factor kappa B subunit 2	0.0487	− 1.432
PRDX1	Peroxiredoxin 1	0.0117	− 1.343
PRDX2	Peroxiredoxin 2	0.0202	− 1.427
PRDX3	Peroxiredoxin 3	0.089	− 1.152
PRDX4	Peroxiredoxin 4	0.0176	− 1.406
PRDX6	Peroxiredoxin 6	0.0244	− 1.733
SOD1	Superoxide dismutase 1	0.0376	− 1.268
SOD2	Superoxide dismutase 2	0.0275	− 1.194
VCAM1	Vascular cell adhesion molecule 1	0.00421	− 1.359

In order to examine the molecular mechanisms, cyclopedic and quantitative comparisons of mRNA expression levels in cerebral infarct lesions between the male WT and triple n/i/eNOSs$^{-/-}$ genotypes at 1 h after MCAO by RNA sequencing were carried out (each $n=4$). Both the canonical pathway analysis and the tox list analysis indicated a significant involvement of oxidative stress and mitochondrial dysfunction (Fig. 5A, B). mRNA levels of 16 genes that are related to oxidative stress were differentially expressed as shown below

The brain is the organ that is most susceptible to oxidative stress, and oxidative stress plays a critical role in the pathogenesis of cerebral infarction [28, 29]. An excess amount of free radicals is produced irrespective of transient or sustained cerebral ischemia, and endogenous anti-oxidative substances (free radical scavengers) are consumed, resulting in neuronal cell injury. In the phase III clinical study, intravenous administration of the free radical scavenger, edaravone, has been shown to improve prognosis of patients with cerebral infarction within 72 h after the onset [31], and edaravone is used in the treatment of an acute phase of cerebral infarction within 24 h after the onset in Japan. Mitochondrial dysfunction has been

Table 2 Differentially expressed genes that are related to mitochondrial dysfunction

Symbol	Gene name	*P* value	Fold change
ACO1	Aconitase 1	0.00553	– 1.225
APP	Amyloid beta precursor protein	0.00494	1.198
ATP5C1	ATP synthase, H+ transporting, mitochondrial F1 complex, gamma polypeptide 1	0.00332	– 1.292
ATP5F1	ATP synthase, H+ transporting, mitochondrial Fo complex subunit B1	0.013	– 1.271
ATP5H	ATP synthase, H+ transporting, mitochondrial Fo complex subunit D	0.0125	– 1.334
ATP5J	ATP synthase, H+ transporting, mitochondrial Fo complex subunit F6	0.0344	– 1.307
ATP5J2	ATP synthase, H+ transporting, mitochondrial Fo complex subunit F2	0.0379	– 1.347
ATP5L	ATP synthase, H+ transporting, mitochondrial Fo complex subunit G	0.0143	– 1.41
ATP5O	ATP synthase, H+ transporting, mitochondrial F1 complex, O subunit	0.0117	– 1.375
ATPAF1	ATP synthase mitochondrial F1 complex assembly factor 1	0.0209	1.226
ATPAF2	ATP synthase mitochondrial F1 complex assembly factor 2	0.0212	– 1.189
BACE1	Beta-secretase 1	0.0207	1.212
BACE2	Beta-site APP-cleaving enzyme 2	0.0139	– 1.736
BCL2	BCL2, apoptosis regulator	0.00215	1.196
CASP3	Caspase 3	0.0853	– 1.273
CASP8	Caspase 8	0.0189	– 2.332
CAT	Catalase	0.000862	– 1.216
COX6B1	Cytochrome c oxidase subunit 6B1	0.0264	– 1.436
Cox6c	Cytochrome c oxidase subunit VIc	0.00483	– 1.445
COX7A2	Cytochrome c oxidase subunit 7A2	0.0214	– 1.372
COX7B	Cytochrome c oxidase subunit 7B	0.0444	– 1.405
CYCS	Cytochrome c, somatic	0.00689	– 1.297
GPX7	Glutathione peroxidase 7	0.00705	– 1.691
MAPK8	Mitogen-activated protein kinase 8	0.000112	– 1.35
MAPK9	Mitogen-activated protein kinase 9	0.026	1.205
MAPK10	Mitogen-activated protein kinase 10	0.0951	1.139
NDUFA1	NADH:ubiquinone oxidoreductase subunit A1	0.0403	– 1.384
NDUFA9	NADH:ubiquinone oxidoreductase subunit A9	0.00964	– 1.273
NDUFA10	NADH:ubiquinone oxidoreductase subunit A10	0.0187	– 1.187
NDUFB3	NADH:ubiquinone oxidoreductase subunit B3	0.00822	– 1.384
NDUFB11	NADH:ubiquinone oxidoreductase subunit B11	0.018	– 1.444
NDUFS4	NADH:ubiquinone oxidoreductase subunit S4	0.0466	– 1.299
NDUFS8	NADH:ubiquinone oxidoreductase core subunit S8	0.00588	– 1.338
NDUFV2	NADH:ubiquinone oxidoreductase core subunit V2	0.0459	– 1.221
NDUFV3	NADH:ubiquinone oxidoreductase subunit V3	0.0407	– 1.332
PINK1	PTEN induced putative kinase 1	0.0123	1.143
PRDX3	Peroxiredoxin 3	0.089	– 1.152
PSEN2	Presenilin 2	0.0376	– 1.195
PSENEN	Presenilin enhancer gamma-secretase subunit	0.0182	– 1.35
SDHA	Succinate dehydrogenase complex flavoprotein subunit A	0.00679	1.115
SOD2	Superoxide dismutase 2	0.0275	– 1.194
UQCRB	Ubiquinol-cytochrome c reductase binding protein	0.00695	– 1.457
UQCRC2	Ubiquinol-cytochrome c reductase core protein 2	0.00522	– 1.244
UQCRQ	Ubiquinol-cytochrome c reductase complex III subunit VII	0.0429	– 1.434
VDAC1	Voltage dependent anion channel 1	0.0367	– 1.112
VDAC2	Voltage dependent anion channel 2	0.028	– 1.192
VDAC3	Voltage dependent anion channel 3	0.034	– 1.217

In order to examine the molecular mechanisms, cyclopaedic and quantitative comparisons of mRNA expression levels in cerebral infarct lesions between the male WT and triple n/i/eNOSs$^{-/-}$ genotypes at 1 h after MCAO by RNA sequencing were carried out (each $n=4$). Both the canonical pathway analysis and the tox list analysis indicated a significant involvement of oxidative stress and mitochondrial dysfunction (Fig. 5A, B). mRNA levels of 44 genes that are related to mitochondrial dysfunction were differentially expressed as shown below

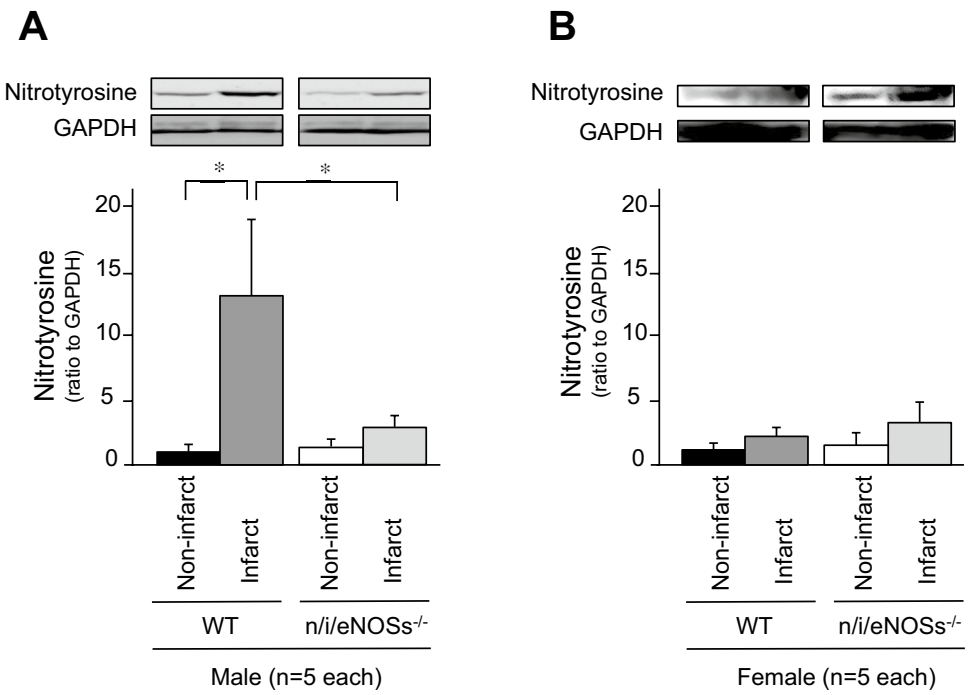

Fig. 6 Western blot analysis of nitrotyrosine in cerebral infarct lesions and non-cerebral infarct regions in male and female WT and triple n/i/eNOSs$^{-/-}$ mice at 24 h after transient MCAO. *$P < 0.05$. The data were analyzed by ANOVA followed by Bonferroni's test

considered as one of the hallmarks of cerebral infarction and contributes to the pathology of cerebral ischemia and reperfusion [29, 30]. Mitochondria is essential in promoting neural survival and neurological improvement following cerebral infarction. Under a condition of cerebral infarction, mitochondrial dysfunction induces reactive oxygen species production, mitochondrial electron transport dysfunction, mitochondria-mediated regulation of inflammasome activation, mitochondrial dynamics and biogenesis, and apoptotic cell death. Based on these lines of evidence, it is conceivable that decreased oxidative stress and reduced mitochondrial dysfunction are involved in the alleviated cerebral infarction in the male triple n/i/eNOSs$^{-/-}$ mice after the transient MCAO. Taken together, it is possible that testosterone mediates those neuroprotective effects in the male triple n/i/eNOSs$^{-/-}$ mice. We, however, do not reveal the switching mechanism by which testosterone exerts the beneficial and deleterious effects in the absence and presence, respectively, of NOSs. This point remains to be examined in future studies.

In conclusions, we were able to demonstrate that cerebral infarction was reduced in the male, but not the female, triple n/i/eNOSs$^{-/-}$ mice after the MCAO through a testosterone-mediated mechanism, elucidating a novel deleterious role of the whole endogenous NOSs system in the pathogenesis of cerebral infarction. Decreased oxidative stress and reduced mitochondrial dysfunction appear to be involved in the reduced cerebral infarction in the male triple n/i/eNOSs$^{-/-}$ mice.

Author contributions HK, MT, HS, KS, and MK designed research; HK, KK, and HY performed research; HK, MT, HS, KS, and MK analyzed data; and HK, MT, and KK wrote the paper. All authors commented on previous versions of the manuscript. All authors read and approved the final manuscript.

Funding This work was supported in part by the JSPS KAKENHI Grant Numbers JP16K09519 and 19K08657.

Declarations

Conflict of interest The authors declare that they have no conflict of interest in this study.

References

1. Goldstein L. Ischemic cerebrovascular disease. In: Crow M, Davidson N, Drazen J, Griggs R, Landry D, Levinson W, Rustgi A, Scheld W, Sopiegel A, editors. Goldman-cecil medicine. 26th ed.: Elsevier; 2020.
2. Smith W, Johnston S, Hemphili J. Ischemic stroke. In: Loscalzo J, AS F, Kasper D, Hauser S, Longo D, Jameson J, editors. Harrison's principles of internal medicine. 21st ed.: Mc Graw Hill; 2022. p. 3335–48.
3. Brindicci C, Kharitonov SA, Ito M, Elliott MW, Hogg JC, Barnes PJ, Ito K. Nitric oxide synthase isoenzyme expression and activity in peripheral lung tissue of patients with chronic obstructive pulmonary disease. Am J Respir Crit Care Med. 2010;181(1):21–30. https://doi.org/10.1164/rccm.200904-0493OC.
4. Tsutsui M, Shimokawa H, Otsuji Y, Yanagihara N. Pathophysiological relevance of NO signaling in the cardiovascular system:

novel insight from mice lacking all NO synthases. Pharmacol Ther. 2010;128(3):499–508. https://doi.org/10.1016/j.pharmthera.2010.08.010.
5. Tsutsui M, Tanimoto A, Tamura M, Mukae H, Yanagihara N, Shimokawa H, Otsuji Y. Significance of nitric oxide synthases: lessons from triple nitric oxide synthases null mice. J Pharmacol Sci. 2015;127(1):42–52. https://doi.org/10.1016/j.jphs.2014.10.002.
6. Huang Z, Huang PL, Ma J, Meng W, Ayata C, Fishman MC, Moskowitz MA. Enlarged infarcts in endothelial nitric oxide synthase knockout mice are attenuated by nitro-L-arginine. J Cereb Blood Flow Metab. 1996;16(5):981–7. https://doi.org/10.1097/00004647-199609000-00023.
7. Huang Z, Huang PL, Panahian N, Dalkara T, Fishman MC, Moskowitz MA. Effects of cerebral ischemia in mice deficient in neuronal nitric oxide synthase. Science. 1994;265(5180):1883–5. https://doi.org/10.1126/science.7522345.
8. Iadecola C, Zhang F, Casey R, Nagayama M, Ross ME. Delayed reduction of ischemic brain injury and neurological deficits in mice lacking the inducible nitric oxide synthase gene. J Neurosci. 1997;17(23):9157–64.
9. Yamamoto S, Golanov EV, Berger SB, Reis DJ. Inhibition of nitric oxide synthesis increases focal ischemic infarction in rat. J Cereb Blood Flow Metab. 1992;12(5):717–26. https://doi.org/10.1038/jcbfm.1992.102.
10. Buisson A, Plotkine M, Boulu RG. The neuroprotective effect of a nitric oxide inhibitor in a rat model of focal cerebral ischaemia. Br J Pharmacol. 1992;106(4):766–7. https://doi.org/10.1111/j.1476-5381.1992.tb14410.x.
11. Suda O, Tsutsui M, Morishita T, Tanimoto A, Horiuchi M, Tasaki H, Huang PL, Sasaguri Y, Yanagihara N, Nakashima Y. Long-term treatment with N(omega)-nitro-L-arginine methyl ester causes arteriosclerotic coronary lesions in endothelial nitric oxide synthase-deficient mice. Circulation. 2002;106(13):1729–35. https://doi.org/10.1161/01.cir.0000029749.16101.44.
12. Suda O, Tsutsui M, Morishita T, Tasaki H, Ueno S, Nakata S, Tsujimoto T, Toyohira Y, Hayashida Y, Sasaguri Y, Ueta Y, Nakashima Y, Yanagihara N. Asymmetric dimethylarginine produces vascular lesions in endothelial nitric oxide synthase-deficient mice: involvement of renin-angiotensin system and oxidative stress. Arterioscler Thromb Vasc Biol. 2004;24(9):1682–8. https://doi.org/10.1161/01.ATV.0000136656.26019.6e.
13. Morishita T, Tsutsui M, Shimokawa H, Sabanai K, Tasaki H, Suda O, Nakata S, Tanimoto A, Wang KY, Ueta Y, Sasaguri Y, Nakashima Y, Yanagihara N. Nephrogenic diabetes insipidus in mice lacking all nitric oxide synthase isoforms. Proc Natl Acad Sci U S A. 2005;102(30):10616–21. https://doi.org/10.1073/pnas.0502236102.
14. Laubach VE, Shesely EG, Smithies O, Sherman PA. Mice lacking inducible nitric oxide synthase are not resistant to lipopolysaccharide-induced death. Proc Natl Acad Sci U S A. 1995;92(23):10688–92. https://doi.org/10.1073/pnas.92.23.10688.
15. Maeda K, Hata R, Hossmann KA. Differences in the cerebrovascular anatomy of C57black/6 and SV129 mice. NeuroReport. 1998;9(7):1317–9. https://doi.org/10.1097/00001756-199805110-00012.
16. Coyle P, Jokelainen PT. Dorsal cerebral arterial collaterals of the rat. Anat Rec. 1982;203(3):397–404. https://doi.org/10.1002/ar.1092030309.
17. Coyle P. Spatial relations of dorsal anastomoses and lesion border after middle cerebral artery occlusion. Stroke. 1987;18(6):1133–40. https://doi.org/10.1161/01.str.18.6.1133.
18. Longa EZ, Weinstein PR, Carlson S, Cummins R. Reversible middle cerebral artery occlusion without craniectomy in rats. Stroke. 1989;20(1):84–91. https://doi.org/10.1161/01.str.20.1.84.
19. Hata R, Mies G, Wiessner C, Fritze K, Hesselbarth D, Brinker G, Hossmann KA. A reproducible model of middle cerebral artery occlusion in mice: hemodynamic, biochemical, and magnetic resonance imaging. J Cereb Blood Flow Metab. 1998;18(4):367–75. https://doi.org/10.1097/00004647-199804000-00004.
20. Manley GT, Fujimura M, Ma T, Noshita N, Filiz F, Bollen AW, Chan P, Verkman AS. Aquaporin-4 deletion in mice reduces brain edema after acute water intoxication and ischemic stroke. Nat Med. 2000;6(2):159–63. https://doi.org/10.1038/72256.
21. Swanson RA, Morton MT, Tsao-Wu G, Savalos RA, Davidson C, Sharp FR. A semiautomated method for measuring brain infarct volume. J Cereb Blood Flow Metab. 1990;10(2):290–3. https://doi.org/10.1038/jcbfm.1990.47.
22. Drel VR, Pacher P, Stevens MJ, Obrosova IG. Aldose reductase inhibition counteracts nitrosative stress and poly(ADP-ribose) polymerase activation in diabetic rat kidney and high-glucose-exposed human mesangial cells. Free Radic Biol Med. 2006;40(8):1454–65. https://doi.org/10.1016/j.freeradbiomed.2005.12.034.
23. Kina-Tanada M, Sakanashi M, Tanimoto A, Kaname T, Matsuzaki T, Noguchi K, Uchida T, Nakasone J, Kozuka C, Ishida M, Kubota H, Taira Y, Totsuka Y, Kina SI, Sunakawa H, Omura J, Satoh K, Shimokawa H, Yanagihara N, Maeda S, Ohya Y, Matsushita M, Masuzaki H, Arasaki A, Tsutsui M. Long-term dietary nitrite and nitrate deficiency causes the metabolic syndrome, endothelial dysfunction and cardiovascular death in mice. Diabetologia. 2017;60(6):1138–51. https://doi.org/10.1007/s00125-017-4259-6.
24. Ogoshi T, Tsutsui M, Kido T, Sakanashi M, Naito K, Oda K, Ishimoto H, Yamada S, Wang KY, Toyohira Y, Izumi H, Masuzaki H, Shimokawa H, Yanagihara N, Yatera K, Mukae H. Protective role of myelocytic nitric oxide synthases against hypoxic pulmonary hypertension in mice. Am J Respir Crit Care Med. 2018;198(2):232–44. https://doi.org/10.1164/rccm.201709-1783OC.
25. Li Y, Zhang J. Animal models of stroke. Animal Model Exp Med. 2021;4(3):204–19. https://doi.org/10.1002/ame2.12179.
26. Hawk T, Zhang YQ, Rajakumar G, Day AL, Simpkins JW. Testosterone increases and estradiol decreases middle cerebral artery occlusion lesion size in male rats. Brain Res. 1998;796(1–2):296–8. https://doi.org/10.1016/s0006-8993(98)00327-8.
27. Wang C, Gong B, Bushel PR, Thierry-Mieg J, Thierry-Mieg D, Xu J, Fang H, Hong H, Shen J, Su Z, Meehan J, Li X, Yang L, Li H, Labaj PP, Kreil DP, Megherbi D, Gaj S, Caiment F, van Delft J, Kleinjans J, Scherer A, Devanarayan V, Wang J, Yang Y, Qian HR, Lancashire LJ, Bessarabova M, Nikolsky Y, Furlanello C, Chierici M, Albanese D, Jurman G, Riccadonna S, Filosi M, Visintainer R, Zhang KK, Li J, Hsieh JH, Svoboda DL, Fuscoe JC, Deng Y, Shi L, Paules RS, Auerbach SS, Tong W. The concordance between RNA-seq and microarray data depends on chemical treatment and transcript abundance. Nat Biotechnol. 2014;32(9):926–32. https://doi.org/10.1038/nbt.3001.
28. Jelinek M, Jurajda M, Duris K. Oxidative stress in the brain: basic concepts and treatment strategies in stroke. Antioxidants (Basel). 2021. https://doi.org/10.3390/antiox10121886.
29. Khoshnam SE, Winlow W, Farzaneh M, Farbood Y, Moghaddam HF. Pathogenic mechanisms following ischemic stroke. Neurol Sci. 2017;38(7):1167–86. https://doi.org/10.1007/s10072-017-2938-1.
30. He Z, Ning N, Zhou Q, Khoshnam SE, Farzaneh M. Mitochondria as a therapeutic target for ischemic stroke. Free Radic Biol

Med. 2020;146:45–58. https://doi.org/10.1016/j.freeradbiomed.2019.11.005.
31. Edaravone Acute Infarction Study G. Effect of a novel free radical scavenger, edaravone (MCI-186), on acute brain infarction. Randomized, placebo-controlled, double-blind study at multicenters. Cerebrovasc Dis. 2003;15(3):222–9. https://doi.org/10.1159/000069318.